

RESEARCH ARTICLE

Analysis of the Integration of a DC-Charging Station Into a Tram Grid by Using Long-Term Field Measurements and a PHiL Setup

THOMAS ESCH^{id}, GERRIT BREMER^{id}, WIEBKE DIRKSEN^{id}, CARLOS MUÑOZ^{id},
AND KARSTEN VON MAYDELL^{id}

Institute of Networked Energy Systems, German Aerospace Center (DLR), 26129 Oldenburg, Germany

Corresponding author: Gerrit Bremer (gerrit.bremer@dlr.de)

This work was supported by German Federal Ministry for Economic Affairs and Climate Action (Bundesministerium für Wirtschaft und Klimaschutz, BMWK) through the Project DC-LEO (Ladeinfrastruktur für Elektromobilität an Oberleitungsnetzen/Charging infrastructure for electromobility on catenary line networks) under Grant no. 01ME20005E.

ABSTRACT The electrification of the transport sector is accompanied by a massive increase of charging infrastructure which is supplied by the public distribution grid. Grid reinforcements and expansions are necessary. This publication investigates an alternative by using an existing DC-electric tram grid as the supply source. For this, long term field measurements of one year at the tram grid of Nordhausen, Germany, are presented. Furthermore, a realistic Power-Hardware-in-the-Loop (PHiL) test environment based on measurement data and a simulation model of the tram grid is realised picturing the highly fluctuating grid behaviour. The simulation model is validated based on the field measurement data and the deviation to measured data is calculated. The PHiL environment is used for tests with a 50 kW charging station demonstrator that performs a complete charging cycle of an emulated electric vehicle (EV). The additional voltage drop and load on the tram grid that is caused by the charging process is shown and compared to a scenario without electric charging.

INDEX TERMS Electric charging, EVSE, electric tram grid, electric tram, DC-grid, field measurement, power-hardware-in-the-loop, real time simulation.

I. INTRODUCTION

The electrification of the transport sector requires increasing integration of electric vehicle supply equipment (EVSE) into the existing electricity grid. By the year 2030, the German government has set the target of one million charging points installed throughout the country [1]. In order to meet this target, reinforcing and expanding the electricity grid might be necessary, although for urban areas the usage of the existing low voltage direct current (LVDC) electric tram grid can be an alternative. Such systems are available in almost 70 cities in Germany. Besides reducing grid reinforcement costs, those charging stations can be configured

as park & ride car parks to reduce the private transport inside the city. Challenging however may be the fluctuating voltage level due to frequent braking and acceleration of the trains.

The capacity of the LVDC grid for electric vehicle (EV) charging was investigated for the city of Edinburgh [2]. Integrating photovoltaic generation and EV charging into the LVDC electric tram grid with an electric management system was introduced in [3]. In [4] overvoltages due to braking were reduced when an EV is being charged thus stabilising the grid voltage. However all aforementioned results were obtained via simulation. Rapid prototyping of DC-DC converters via a Power-Hardware-in-the-Loop (PHiL) environment has been carried out in [5], [6], and [7] for different DC grid applications.

The associate editor coordinating the review of this manuscript and approving it for publication was Jahangir Hossain^{id}.

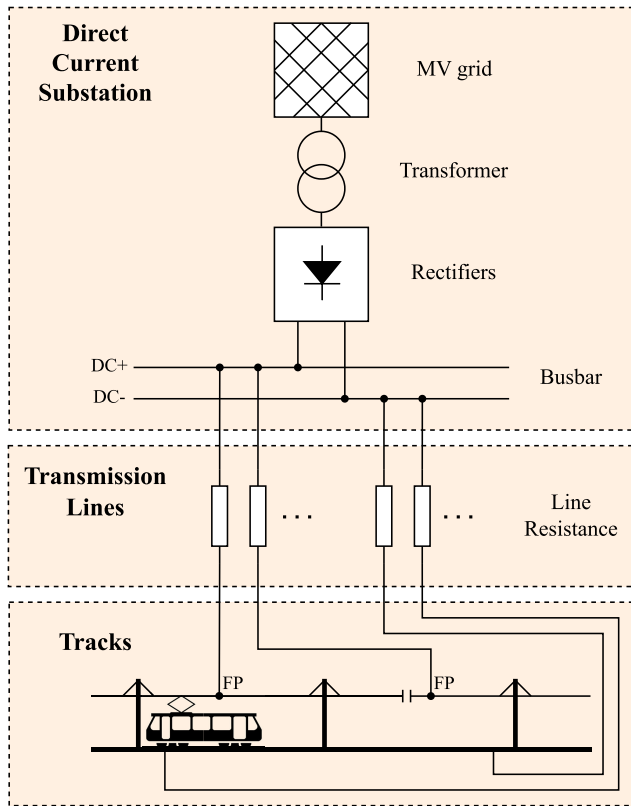


FIGURE 1. Overview of the electric grid of the tram system.

This paper investigates the integration of a DC-DC charging station demonstrator into the fluctuating electric tram grid of Nordhausen, Germany simulated in a PHiL context. The utilised laboratory environment was explained by Maydell et al. [8]. At first an introduction to the tram grid in Nordhausen is given as well as long term field measurement data of the system in Section II. In Section III the set-up of the simulink model of the tram grid system is explained and validated. The simulation model is integrated into a PHiL laboratory environment via a real time system. Section IV explains the results obtained from the laboratory tests while the conclusion of this work is found in Section V.

II. FIELD MEASUREMENTS

In order to investigate the electric behaviour of a tram grid system, a long term field measurement was conducted in the German city of Nordhausen. The electric tram grid system in Nordhausen consists of two tramlines. Tramline 1 is 3.2 km long and connects the north with the south, while tramline 2 (4.6 km long) connects the east with the west side of the city. Up to seven trains are on the tracks at the same time [9]. In this section, the measurement set-up as well as the analysis of the obtained measurement data is described.

A. DESCRIPTION OF THE ELECTRIC TRAM GRID

Fig. 1 provides an overview of the electric DC grid of the tram system in Nordhausen. The alternating medium voltage (MV)

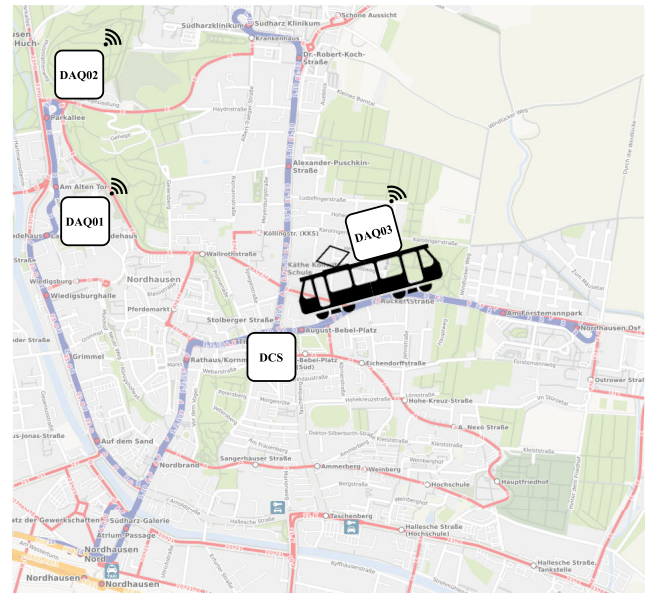


FIGURE 2. Placement of the DAQ units along the tram line of Nordhausen, Germany marked in blue.

of the public grid is transformed and rectified in the direct current substation (DCS) via transformers and unidirectional passive rectifiers, whereby the nominal DC voltage is 660 V. A network of transmission lines connected to the DCS busbar system distributes the energy via several feed points (FP) to the catenary line along the railway tracks. However, the catenary line is divided into segments so that each FP is electrically separated from the others. The tracks on the ground are the common return which are non-separated but connected via a different network of transmission lines with the busbar system at the DCS. As the tram trains are the main electric loads in the grid and are moving along the track, the position of the electrical loads in the network varies over time. This is exceptional to other electricity grids.

B. DATA ACQUISITION

For generating information of the electric behaviour of the tram grid, three data acquisition (DAQ) units were installed in the grid for approximately one year. Fig. 2 shows their position along the two tram lines in Nordhausen marked in blue.

Two units, DAQ01 and DAQ02, are installed stationary and measure the voltage via LEM DVC 1000-B voltage sensors. A third unit, DAQ03, is installed on top of a tram train and measures its voltage as well as its current along the route via an additional LEM HOP 1500-SB current sensor. The measured data is send to a server using mobile communication.

The stationary unit DAQ02 is installed the furthest away from the DCS with a total line length of approximately 3 km. At this installation point, the highest voltage fluctuations due to the high line resistance are expected. Unit DAQ01 is installed at the tram depot where the line distance between the

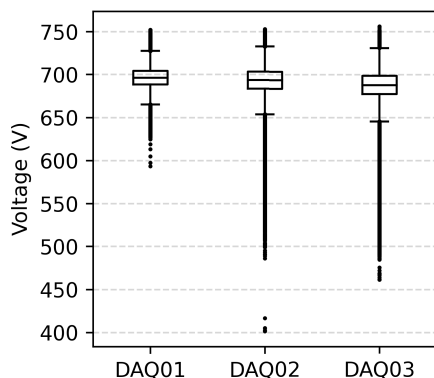


FIGURE 3. Boxplot for the voltage measurements of the DAQ units.

DCS and the FP dedicated only for the depot is approximately 2.2 km. However due to only slight loads at the tram depot during the operating hours, the voltage drop over the line between the DCS and the measurement point is expected to be insignificant. Therefore the transmission line resistance between the FP of the depot and the DCS is expected to have less effect on the voltage measurement resulting in an electrically close measurement of the voltage at the DCS despite a geographically deviating position of the depot.

C. FIELD DATA PRESENTATION

The data acquisition period for the DAQ units ranges from April 30, 2021 until August 30, 2022. The mean voltage measurements for the three DAQ units are summarised and depicted as boxplots in Fig. 3, with a resolution of five seconds for units DAQ01 and DAQ02, and one second for unit DAQ03.

The boxplots depict the five-number summary of the dataset:

- Minimum measurement
- 25th percentile
- Median
- 75th percentile
- Maximum measurement

The lower and upper line of the rectangle represent the 25th percentile (lower quartile) and 75th percentile (upper quartile), respectively. The middle line represents the median of the dataset. Following the distance of 1.5 times the Interquartile Range (distance between the upper and lower quartile), the upper whisker extends until the largest measurement that is within this distance, and the lower whisker extends until the smallest measurement that is within this distance. All measurements that are outside of this range are shown as outliers as dots. The median voltage values are 696 V for unit DAQ01, 693 V for unit DAQ02 and 687 V for unit DAQ03. These values show that the measured system voltage is higher than the nominal voltage of 660 V of the tram grid. The nominal voltage declaration was defined with first use of the grid and is not monitored for operational reasons in detail.

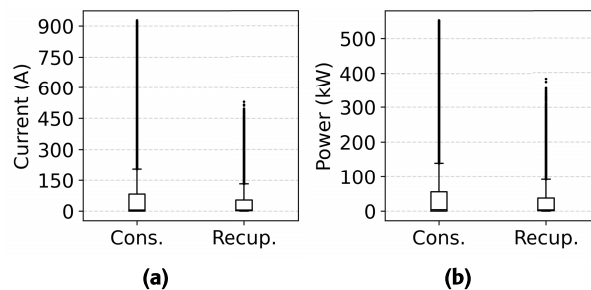


FIGURE 4. Boxplot of the consumption and recuperation measured by the DAQ03 unit. (a) Measured current. (b) Measured power.

It can be seen that the voltage readings of the units DAQ02 and DAQ03 shows a wider range compared to unit DAQ01. For instance, most of the five-number summary values of unit DAQ02 are lower than for the unit DAQ01, and most of the five-number summary values of unit DAQ03 are lower than for the unit DAQ02. This is due to the fact that unit DAQ02 is located on a position far away from the DCS, so the line resistance cause a higher voltage drop. Moreover, as DAQ03 is located on a tram, the measurement shows the voltage behaviour along the whole track of the electrical load and therewith shows the widest voltage range. Additionally, at each DAQ unit, voltage peaks were measured. This is due to the recuperation of the trams during deceleration events, as braking energy is fed back from the tram to the grid.

The measured mean current of DAQ03 and its power calculated as the product of voltage and current are shown in Fig. 4 as boxplots based on data with a time resolution of one second. The plots are separated for reasons of clarity, each showing a boxplot for energy consumption and recuperation of the tram. Therefore only positive values are shown in the plot. Consumption depicts the situation when the energy flows from the grid to the tram, while recuperation denotes energy flowing from the tram to the grid. For the current consumption boxplot seen in Fig. 4a, the upper quartile is at 82 A and the maximum value is at 206 A; for the current recuperation, the upper quartile is at 54 A and the maximum value is at 132 A. For the power consumption boxplot in Fig. 4b, the upper quartile is at 56 kW and the maximum is at 139 kW; for the power recuperation boxplot, the upper quartile is at 38 kW and the maximum value is 92 kW. For all four boxplots, outliers shown as black dots indicate high temporarily peaks of the current and power of the tram.

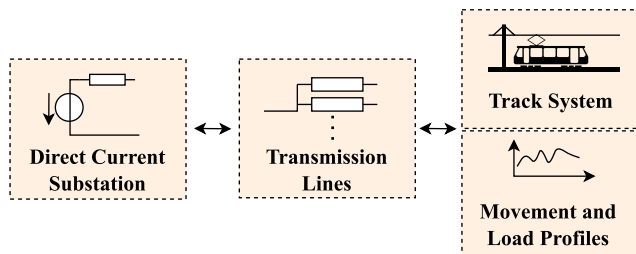
As Fig. 3 and Fig. 4 depict mean values with time resolutions of five seconds and one second, maximum values are not captured. Measured maximum values, as well as the timestamp of the occurrence can be seen in Table 1. The timestamp is shown in the format year-month-day hour:minute:second.

III. SIMULATION MODEL AND PHIL-ENVIRONMENT

Based on the information of the tram grid in Nordhausen shown in section II-A, an electrical simulation model is

TABLE 1. Maximum values for the voltage, current and power for each DAQ unit.

Unit	Parameter	Value	Timestamp
DAQ01	Voltage	922 V	2022-03-06 22:25:20
DAQ02	Voltage	926 V	2022-03-06 22:25:20
	Voltage	815 V	2021-07-31 09:42:50
	Current Cons.	1273 A	2021-08-29 17:26:55
DAQ03	Current Recup.	531 A	2021-10-11 06:36:40
	Power Cons.	551 kW	2021-07-29 07:14:30
	Power Recup.	381 kW	2021-10-11 06:36:39

**FIGURE 5.** Overview of the simulation model structure.

realised using a Simulink Simscape Electrical environment. Therewith a digital twin of the tram grid is set up, which is able to generate a real time laboratory test environment for the charging station demonstrator.

A. MODEL STRUCTURE AND ASSUMPTIONS

Fig. 5 provides an overview of the simulation model structure. It consists of four main parts: the DCS, the transmission lines, the track and the overall control algorithm.

The first part is the DCS supplying the grid voltage. It is simplified by using a DC voltage source with a serial resistance for generating a load depending behaviour. The serial resistance is based on the internal resistance of the medium voltage transformer used in the direct current substation.

In the second part of the model, the transmission lines between the DCS and the FPs of the tram grid are modelled by using electrical resistances. Their input parameters are the particular length and cross-section of each line.

Third, the main part of the model covers the track system itself. Therefore the main track is divided into grid segments that each represent a part of the track of varying length depending on local circumstances such as track switches, catenary line separators or FPs. Due to the fact that the positions of these track equipments along the track are mostly known, the distance between two of them defines one grid segment. Each grid segment is modelled with an electrical connection for both, the catenary line and the track, by using resistances defined by the related length and conductivity.

In comparison to other electrical grids, the electrical loads are not connected at one fixed connection point in the

considered tram grid. Instead the trams, as they are the main electric loads, are continually changing their position inside the grid while driving on the track. In the model, this behavior is taken into account by implementing a controlled current source in each grid segment connected between the catenary line and the track. Therewith the fluctuating load current from the trams at each particular grid position can be set.

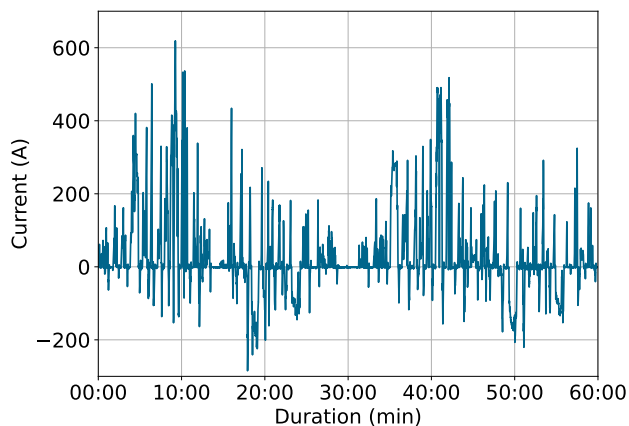
The control of the current sources is implemented by an overlaid control algorithm, the fourth part of the model. This calculates the position of each tram on the track system and assigns its actual current value to it. Therefore the trams are evenly distributed along the track with respect to the length of the line track and the number of trams at the respective line. This leads to the fact, that it is not excluded for two trams being in the same grid segment at the same time (virtual accidents). Additionally there is a deviation of the simulated position to the real train schedule, since stops of trams during their way along the track are not taken into account.

For a most realistic load behaviour of the trams used in the model, the applied current profiles are datasets extracted from the measurement data of the DAQ units. For each line there is a profile covering two complete laps on the track. The total time is adapted to the nominal lap time of 30 minutes for line 1 and 40 minutes for line 2. Fig. 6 shows the used current profiles for the simulation. The control algorithm uses for each tram on the same line the same current profile but with a time shift regarding the position of each tram on the track.

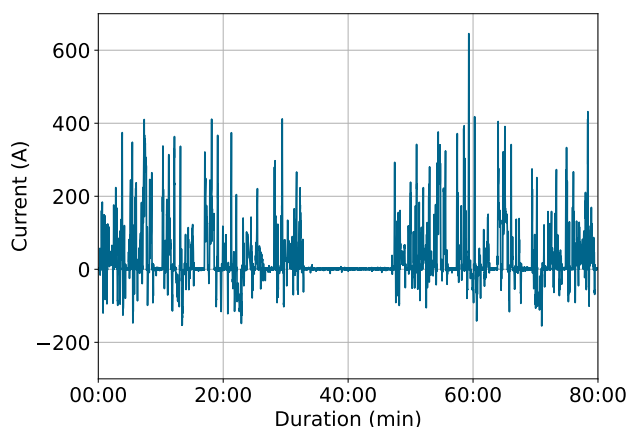
B. MODEL VALIDATION

As described, several details of the real tram grid are not known and during modelling assumptions are made. For qualifying the error between simulated environment and real tram grid, investigations for validation are made.

Therefore the current profiles for line 1 and line 2 are used to simulate the tram grid using the described simulation model. Following this, the simulation output - the applied voltage at the trams during their way through the track - is compared with the measured DAQ unit data, namely the voltage related to the current profiles. The result is shown in Fig. 7a) for line 1 and Fig. 7b) for line 2 as a graph of the tram voltage. The measured voltage of the DAQ03 unit is shown in blue, while the simulation output is shown as a dashed green graph. Because of assumptions during modelling and the unknown number and behaviour of active trams in the real grid, which are affecting the measured voltage, a difference between measurement and simulation is expected. The deviation can partly be seen as a static offset at the simulation indicating the simulated grid is stronger than the real grid. Besides, the graphical comparison shows the measured dataset is characterised by a greater noise on the voltage signal. Reasons for that are the assumption of an ideal DC source instead of a passive rectifier as well as the unknown behaviour and position of the trams on the track. Also, the position of the considered tram is not matched to a real lab round, as described in section III-A.



(a)



(b)

FIGURE 6. Current profiles. (a) Line 1. (b) Line 2.

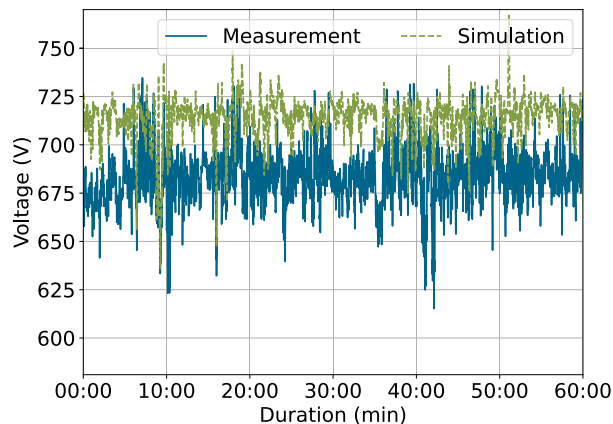
For qualification, the Root-Mean-Square Error (RMSE), the Normalized-RMSE (NRMSE) and the Mean-Absolute-Error (MAE) are calculated as shown in Eq. 1 to 3.

$$RMSE = \frac{\sqrt{\sum_{i=0}^n (A_i - B_i)^2}}{n} \quad (1)$$

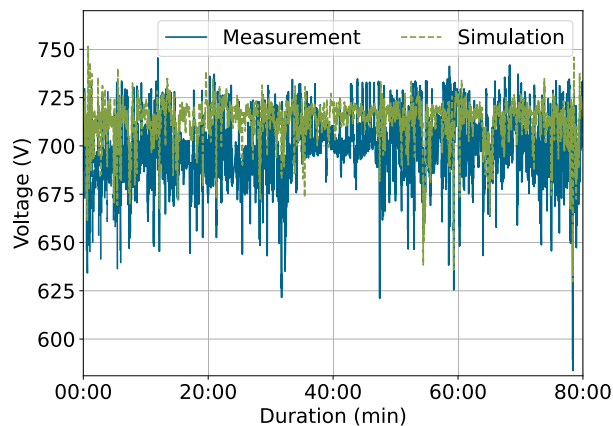
$$NRMSE = \frac{RMSE}{\frac{\sum_{i=0}^n A_i}{n}} \quad (2)$$

$$MAE = \frac{\sum_{i=0}^n |A_i - B_i|}{n} \quad (3)$$

With n as number of samples of the timeline, A_i and B_i as the single timeseries values of the measured and simulated data. The results are shown in Table 2. The errors of the currents at line 1 and 2 should ideally be 0, as they are the same dataset. Nevertheless, a small error is existing, that can be attributed to uncertainties of the real laboratory environment and measurement inaccuracies. Comparing the voltages as the result of this validation, the error is existing but



(a)



(b)

FIGURE 7. Simulated and measured tram voltages. (a) Line 1. (b) Line 2.

TABLE 2. Overview of the different error types of the model validation.

Results	RMSE	NRMSE	MAE
Current Line 1	0.15 A	0,5 %	0.14 A
Voltage Line 1	33.2 V	4,9 %	30.6 V
Current Line 2	0.15 A	0,6 %	0.14 A
Voltage Line 2	21.6 V	3,1 %	15.9 V

small enough showing that the simulation model is suitable for generating a realistic picture of the real tram grid.

C. LABORATORY SETUP

With the integration of the simulation model in the laboratory environment, a PHiL-configuration is set up. Fig. 8 shows an overview of the setup.

The simulated tram grid model is running on a Speedgoat real-time system with a step-size of 350 μ s generating the control signal for a cluster of five Delta Electronics SM15k DC sources. They provide the fluctuating DC grid voltage and therewith emulate the behaviour of the tram grid at the planned installation position of the charging station

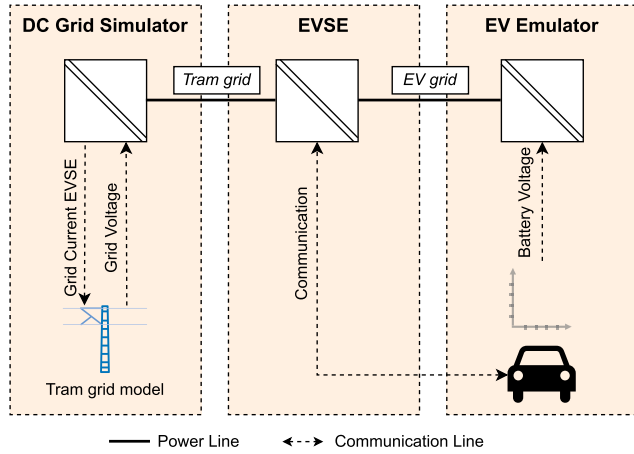


FIGURE 8. Overview of the laboratory setup.

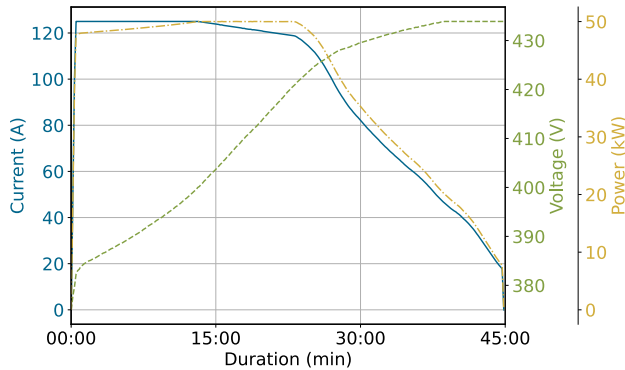


FIGURE 9. Charging curve of the EV.

demonstrator which is located approximately 600 m away from the position of DAQ02. Additionally, the grid current of the charging station is send back to the simulation model creating a corresponding electric load in the model, which generates a feedback loop.

The EVSE is supplied by this grid emulation and provides the charging current for the EV, which is also emulated by another cluster of five Delta Electronics SM15k DC sources configured as sinks thus providing the battery voltage of the charging car.

The battery of the EV is emulated by a battery charging behaviour as shown in Fig. 9. The characteristics of the emulated battery are shown in Table 3. The predefined charging current requested by the EV rises to its maximum value of 125 A at the start of the charging process and reduces with increasing State of Charge (SoC). The charging voltage provided by the vehicle simulator, on the other hand, increases with time.

Electrical measurements during the tests are done with a DEWESoft SIRIUS-HV-system with current sensors LEM IT 200-S ULTRASTAB measuring at 2 kHz sample rate. Input and output currents and voltages of the charging station demonstrator are measured.

TABLE 3. Parameters of the emulated battery.

Parameter	Value
max. charging power	50 kW
max. charging current	125 A
nominal battery voltage	400 V
charged energy	30 kW h

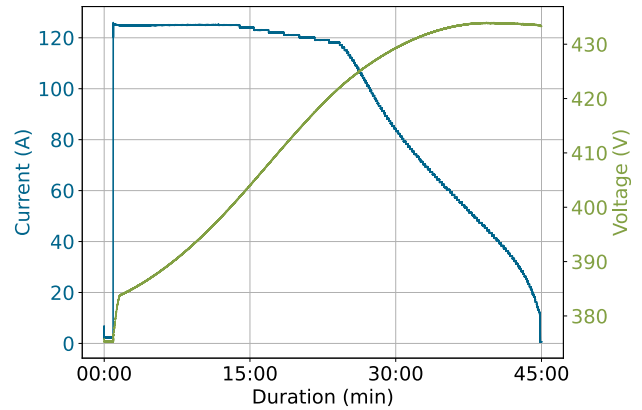


FIGURE 10. Measured charging current and voltage of the EV during the laboratory test.

IV. PHIL TEST RESULTS

Using the PHIL setup described in section III, charging tests are realised. The results are discussed in this chapter.

Fig. 10 shows the measured values of the EV charging voltage and current, showing the specified charging process is realised as it matches the battery charging specification (Fig. 9). The battery voltage rises with increasing SoC up to its maximum at 433 V while the battery current also shows the determined behaviour reaching its maximum of 125 A at the beginning of the charging process. The fluctuating grid voltage at the connection point is completely compensated on the EV site by the charging station demonstrator.

In order to investigate the behaviour and impact of a charging process on the tram grid, a comparison is done. Therefore, two cases are considered. Case 1 describes the laboratory tests including the active charging process, while, in case 2, the EVSE is not active. In both cases the simulation of the tram grid includes the maximum number of seven active trams in the grid.

The grid voltage over time for case 1 and case 2 at the connection point of the EVSE is displayed in Fig. 11. The active charging period is indicated by the grey area. It can be seen, that in case 1 the active EVSE causes an additional voltage drop during the charging process.

Fig. 12 shows the voltages at the connection point of the EVSE and at the DCS for each case. Referring to the median values, the charging process generates an average voltage drop at the EVSE of 2,1 % in case 1 compared to case 2 affecting the complete area supplied by the particular

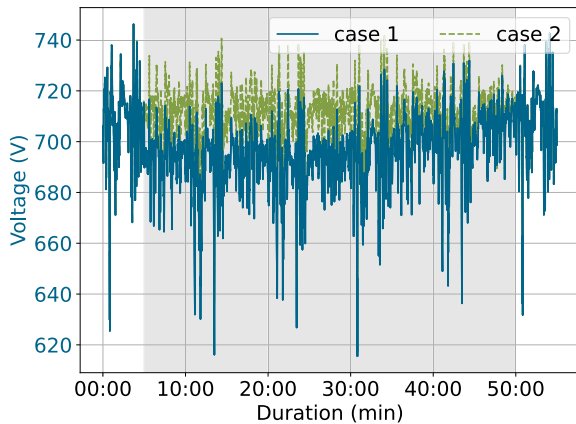


FIGURE 11. Comparison of the EVSE supply voltage with (case 1) and without (case 2) an active charging process. The grey area indicates the charging period for case 1.

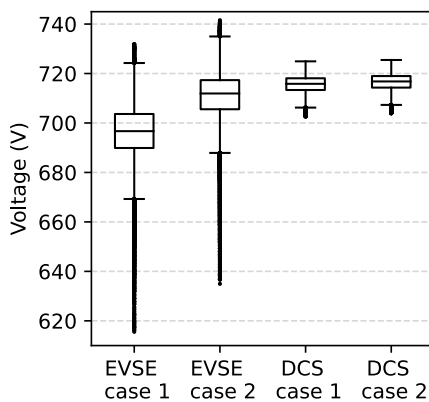


FIGURE 12. Boxplot of the voltage at the connection point of the EVSE with (case 1) and without (case 2) a charging process.

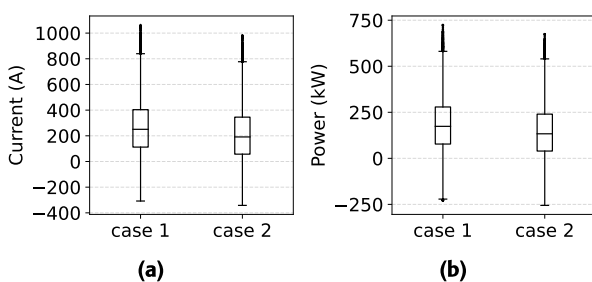


FIGURE 13. Boxplot of the total grid current and power at the connection point of the EVSE with (case 1) and without (case 2) a charging process. (a) Current. (b) Power.

FP (median voltage case 1: 697 V and case 2: 712 V). The impact of the charging process at the DCS is with 0,1 % voltage drop quite small (median voltage case 1: 716 V and case 2: 717 V).

Analysing the additional load on the tram grid due to the charging process, the total current and power of all active loads in the grid are summed up. For case 1 these are seven active trams and the EVSE, while for case 2 only the active

trams apply. Fig. 13 depicts the total current and power in form of boxplots during the time of the charging process. The median total current in the grid increases by 31 % when the EV is being charged (median total current case 1: 251 A and case 2: 191 A). A particular stress in this demonstrated application are short peak currents caused by the trams. The total maximum current in case 1 is 1063 A and 981 A in case 2. The median total power load is increased from 133 kW in case 2 to 174 kW in case 1.

V. CONCLUSION

Within the scope of emulating an EVSE connected to a DC tram grid, this work presents long term field measurements, electrical simulations and a PHiL environment of the tram grid Nordhausen. Thereby the key results are:

- Field measurement data of the tram grid and of a tram within the scope of one year show a significant voltage and load deviation with high outliers depending on the position indicating a highly fluctuating grid.
- The simulation of the electric tram grid using the measured current consumption of the tram along the tracks, shows a maximum NRMSE of 4.8 % for the voltage compared to the measurement data.
- As a use case a realistic PHiL environment based on the simulated grid is set up in which a DC-DC-EVSE is integrated. The charging process of an EV results in an additional voltage drop at the connection point due to the higher line loading. The charging curve of the EV was however not effected by the fluctuations of the tram grid.

Having proven the concept of integrating EVSE into the DC tram grid, in a next step field tests should be done.

Based on the results, further work using the PHiL environment is needed to ensure that the voltage deviation remains within the respective voltage tolerance for tram grids, especially when increasing the charging power or number of EVSE. This may be achieved by integrating a battery storage into the charging station. Moreover, an overall load management could be implemented for that purpose which could also be used for preventing grid overload or to stabilise the grid voltage.

ACKNOWLEDGMENT

The authors would like to thank Stadtwerke Nordhausen—Holding Für Versorgung und Verkehr GmbH and Verkehrsbetriebe Nordhausen GmbH for providing information on the tram grid and accompanying the field measurements in Nordhausen, Germany, and the System Entwicklung Nordhausen GmbH, for assisting the laboratory tests with the charging station demonstrator.

REFERENCES

- [1] Federal Government. (2023). *Masterplan Ladeinfrastruktur II Der Bundesregierung*. Accessed: Jul. 5, 2023. [Online]. Available: https://bmdv.bund.de/SharedDocs/DE/Anlage/G/masterplan-ladeinfrastruktur-2.pdf?__blob=publicationFile

- [2] K. Smith, L. Hunter, S. Galloway, C. Booth, C. Kerr, and M. Kellett, "Integrated charging of EVs using existing LVDC light rail infrastructure: A case study," in *Proc. IEEE 3rd Int. Conf. DC Microgrids (ICDCM)*, May 2019, pp. 1–7, doi: [10.1109/ICDCM45535.2019.9232726](https://doi.org/10.1109/ICDCM45535.2019.9232726).
- [3] J. Pouget, B. Guo, L. Bossoney, J. Coppex, D. Roggo, and C. Ellert, "Energetic simulation of DC railway micro-grid interconnecting with PV solar panels, EV charger infrastructures and electrical railway network," in *Proc. IEEE Vehicle Power Propuls. Conf. (VPPC)*, Gijon, Spain, Nov. 2020, pp. 1–7, doi: [10.1109/VPPC49601.2020.9330829](https://doi.org/10.1109/VPPC49601.2020.9330829).
- [4] B. Guo, J. Pouget, L. Bossoney, M. Carpita, T. Meier, and J.-P. Maye, "Catenary overvoltage stabilization of DC railway electrical system by integrating EV charging stations," in *Proc. 20th Int. Conf. Harmon. Quality Power (ICHQP)*, Naples, Italy, May 2022, pp. 1–6, doi: [10.1109/ICHQP53011.2022.9808815](https://doi.org/10.1109/ICHQP53011.2022.9808815).
- [5] L. Bourserie, A. Zama, L. Chédot, P. Dworakowski, S. Silvant, J. Maneiro, C. M. de Vienne, and V. S. Gómez, "Power hardware in-the-loop validation of DC–DC power converter for offshore wind energy," in *Proc. 21st Eur. Conf. Power Electron. Appl. (EPE ECCE Europe)*, Genova, Italy, Sep. 2019, pp. P.1–P.10, doi: [10.23919/EPE.2019.8914856](https://doi.org/10.23919/EPE.2019.8914856).
- [6] D. Dong, L. Garces, M. Agamy, Y. Pan, X. Wu, H. She, H. Xu, X. Li, and J. Dai, "Control and operation of medium-voltage high-power bidirectional resonant DC–DC converters in shipboard DC distribution systems," in *Proc. IEEE Energy Convers. Congr. Expo. (ECCE)*, Milwaukee, WI, USA, Sep. 2016, pp. 1–9, doi: [10.1109/ECCE.2016.7854958](https://doi.org/10.1109/ECCE.2016.7854958).
- [7] A. Ali, N. Faisal, Z. Zia, I. Makda, and A. Usman, "Rapid prototyping of bidirectional DC–DC converter control using FPGA for electric vehicle charging applications," in *Proc. IEEE 13th Int. Symp. Power Electron. Distrib. Gener. Syst. (PEDG)*, Kiel, Germany, Jun. 2022, pp. 1–6, doi: [10.1109/PEDG54999.2022.9923288](https://doi.org/10.1109/PEDG54999.2022.9923288).
- [8] K. von Maydell, J. Petznik, H. Behrends, T. Esch, M. Ahmed, A. Rubio, L. Uhse, R. Völker, S. Unglaube, S. Geißendörfer, F. Schultdt, and C. Agert, "The networked energy systems emulation center at the German aerospace center DLR—Bridging the gap between digital simulation and real operation of energy grids," *Automatisierungstechnik*, vol. 70, no. 12, pp. 1072–1083, Dec. 2022, doi: [10.1515/AUTO-2022-0019](https://doi.org/10.1515/AUTO-2022-0019).
- [9] Verkehrsbetriebe Nordhausen. (2023). *Zahlen, Daten, Fakten Und Technische Details Combino Duo Straßenbahn*. Accessed: Sep. 10, 2023. [Online]. Available: <https://www.stadtwerke-nordhausen.de/verkehr/busstrassenbahn/zahlen-und-fakten>

THOMAS ESCH received the B.Sc. and M.Sc. degrees in electrical engineering from Karlsruhe University of Applied Sciences, Karlsruhe, Germany, in 2020.

From 2020 to 2023, he was a Research Scientist with the Institute of Networked Energy Systems, German Aerospace Center (DLR), Oldenburg, Germany.

GERRIT BREMER received the B.Sc. and M.Sc. degrees in electrical engineering from the Technical University of Brunswick, Brunswick, Germany, in 2016 and 2018, respectively.

Since 2018, he has been a Research Scientist with the Institute of Networked Energy Systems, German Aerospace Center (DLR), Oldenburg, Germany. His research interests include the development and investigation of applied electrical systems, with a focus on power electronics.

WIEBKE DIRKSEN received the B.Eng. degree in electrical engineering from the Jade University of Applied Sciences, Wilhelmshaven, Germany, in 2020, and the M.Sc. degree in electrical engineering from Technical University Brunswick, Brunswick, Germany, in 2023. She is currently pursuing the Ph.D. degree with the Institute of Networked Energy Systems, German Aerospace Center (DLR), Oldenburg, Germany.

The bachelor studies were conducted in cooperation with the wind turbine manufacturer ENERCON, where she worked from 2016 to 2020. Her research interests include wind and solar energy systems and their integration into the electric grid in order to allow a safe and stable operation.

CARLOS MUÑOZ was born in Panama City, Panama, in 1994. He received the B.Sc. degree in electromechanical engineering from the Technological University of Panama (UTP), Panama City, in 2018, the M.P.M. degree from the Interamerican University of Panama (UIP), Panama City, in 2020, and the M.Sc. degree in sustainable renewable energy technologies (SuRE) from the Carl von Ossietzky University of Oldenburg, Oldenburg, Germany, in 2022.

From 2018 to 2020, he was a Trainee with AES Corporation, where he rotated at the Departments of Commercial, Finance, Business Development, Operations of Power Plants, and Human Resources. He was a Student Assistant with the OFFIS—Institute for Information Technology. Since 2023, he has been a Research Assistant with the Institute of Networked Energy Systems, German Aerospace Center (DLR), Oldenburg. His research interests include energy system dispatch optimization, metal hydride storage, and sector coupling with hydrogen.

KARSTEN VON MAYDELL received the M.Sc. degree in physics from the University of Oldenburg, Oldenburg, Germany, in 2000, and the Ph.D. degree in physics from the University of Marburg, Marburg, Germany, in 2003.

Afterwards, he was a Postdoctoral Researcher in research institutes and as the Project Manager in the industry. Since 2017, he has been the Head of the Energy Systems Technology Department, Institute of Networked Energy Systems, German Aerospace Center (DLR), Oldenburg. His research interests include the design of energy systems, smart energy management for grid connected and off-grid connected systems, integration of flexibilities in energy systems, and robust operation of power grids.

...